GEOPHYSICAL RESEARCH LETTERS, VOL. 38, L23805, doi:10.1029/2011GL049785, 2011

The driving of baroclinic anomalies at different timescales

Javier Blanco-Fuentes[1] and Pablo Zurita-Gotor[1]

Received 25 September 2011; revised 2 November 2011; accepted 3 November 2011; published 13 December 2011.

[1] This work investigates the internal variability of zonal-mean baroclinicity over the Southern Hemisphere midlatitudes. The first two leading modes describe a meridional baroclinicity shift and a sharpening/broadening of baroclinicity, with the shift becoming more dominant at low frequency. The lifecycles of the baroclinic anomalies, estimated by means of lagged regression analysis, are qualitatively different depending on the frequency range. At high frequency, the zonal-mean baroclinicity simply responds to the fast eddy heat flux forcing. At low frequency, the baroclinicity shift is forced by the eddy momentum flux through an eddy driven mean meridional circulation and damped diabatically. The meridional eddy heat flux by planetary scale eddies also contributes to the low-frequency shift but the synoptic eddy heat flux behaves diffusively and damps the baroclinicity anomalies at low frequency. **Citation:** Blanco-Fuentes, J., and P. Zurita-Gotor (2011), The driving of baroclinic anomalies at different timescales, *Geophys. Res. Lett.*, *38*, L23805, doi:10.1029/2011GL049785.

1. Introduction

[2] It is well known that the transient perturbations that dominate the heat and momentum transport in the extratropics grow at the expense of the available potential energy implied by the horizontal temperature gradient in the mean flow [*Lorenz*, 1955]. This temperature gradient, or baroclinicity, plays a pivotal role for eddy development in linear instability theories [*Lindzen and Farrell*, 1980] and in nonlinear models of geostrophic turbulence [*Held and Larichev*, 1996]. The relevance of baroclinicity for eddy growth is also apparent in observations, which show that the most intense eddy activity tends to occur over regions where this parameter is maximized [*Hoskins and Valdes*, 1990; *Nakamura et al.*, 2004].

[3] The processes determining the climatological baroclinicity are also well recognized [see, e.g., *Hartmann*, 1994]. The mean baroclinicity is determined from the balance between the diabatic processes that force it (possibly including latent processes, as discussed by *Hoskins and Valdes* [1990]) and the eddy meridional heat fluxes that smooth it. The eddy momentum fluxes also contribute to regenerating the extratropical baroclinicity through adiabatic cooling and heating in the eddy-driven Ferrel cell [*Robinson*, 2006], being smaller than the other two terms but not negligible. In contrast, the relation between baroclinicity and eddy activity in the time-dependent problem has received much less attention, most of it before the reanalysis era. *Lorenz* [1979] distinguished between "forced and free variations of climate", depending on whether variations in the eddy heat flux and baroclinicity were positively or negatively correlated, respectively. He found evidence for the former in the slow, seasonal scales [see also *Stone and Miller*, 1980] but not for faster timescales. *Stone et al.* [1982] examined the lagged correlation between eddy heat flux and baroclinicity in high frequency data and found a significant (negative) correlation when the former leads but no evidence of eddy heat flux intensification following instances of large baroclinicity.

[4] While these early studies focused on the role of the eddy heat flux for baroclinicity, it has been noted in recent years that much of the extratropical internal variability is driven by processes in the upper troposphere. *Lorenz and Hartmann* [2001, hereinafter LH01] examined the variability of extratropical zonal-mean zonal wind in the Southern Hemisphere and found as the leading mode (the "zonal index") a meridional shift with equivalent barotropic structure, driven by the eddy momentum flux. This meridional shift represents the wind signature of the annular mode variability [*Thompson and Wallace*, 2000], being associated with similar shifts in other dynamical variables and fluxes. In particular, the vertical shear in the leading zonal-wind EOF of LH01 implies that the baroclinicity must also shift following the barotropic wind shift. *Robinson* [2000] attributes the generation of baroclinicity during the zonal index cycle to the effect of surface friction on the anomalous barotropic wind. He also argues that this may enhance the persistence of the zonal index through a positive feedback loop when eddy generation and eddy-induced acceleration respond linearly to the baroclinic anomaly [see also LH01; *Robinson*, 2006].

[5] Thus, two scenarios for baroclinic variability appear plausible. If the variability were dominated by the eddy heat flux, one might expect a pulsing variability in which baroclinicity is weakened during eddy lifecycles [*Simmons and Hoskins*, 1978] and slowly restored during quiescent periods. In contrast, if the eddy momentum flux were driving the variability a meridional shift of baroclinicity might be expected to dominate following the barotropic jet shift. The goal of this work is to assess which of the two scenarios is more relevant for the internal variability of zonal-mean baroclinicity and to investigate more generally what processes contribute to the growth and decay of baroclinic anomalies as a function of the timescale considered. We use for this study Southern Hemisphere (SH) data because of its higher degree of symmetry.

2. Data Analysis and Conventions

[6] We have used for this study daily data on constant pressure levels taken from the National Center for Environmental Prediction (NCEP) reanalysis [*Kalnay et al.*, 1996]

[1]Departamento de Geofísica y Meteorología, Facultad de Ciencias Físicas, Instituto de Geociencias, Universidad Complutense de Madrid, CSIC, Madrid, Spain.

0094-8276/11/2011GL049785

during the full years 1978–2010. Although this data is known to suffer from some deficiencies over the middle and high Southern latitudes due to a misallocation in the assimilation procedure known as PAOBS (see http://wesley.ncep.noaa.gov/paobs/paobs.html), the analysis is unchanged when using Reanalysis-2 data [*Kanamitsu et al.*, 2002], devoid of that problem.

[7] Following LH01, we analyze continuous (full year) data instead of individual seasons. We subtract the mean seasonal cycle (defined here as the first 4 harmonics of the daily climatology) from the daily data to compute daily anomalies. For the EOF analysis, the gridded data was weighted by the square root of mass to make the contribution of each gridpoint to the covariance matrix proportional to its mass. For the purpose of this study, the baroclinicity is defined as the reverse of the zonal-mean meridional potential temperature gradient (to make it positive). Other variables are standard. Eddy variables (denoted with a prime) refer to deviations from the instantaneous zonal mean (denoted with a bar). For some analyses the data (either daily anomalies or daily eddy fluxes) was filtered using a Lanczos filter with 31 weights [*Hamming*, 1989].

[8] Finally, the spectra and cospectra presented in this paper are averages of the 93 spectral realizations available when the full 12045 day timeseries is divided into 256-day long segments, with a 128-day overlapping between them and tapering with a Hanning window.

3. Modes of Baroclinic Variability

[9] Figure 1 describes the climatology and variability of the zonal-mean extratropical (30-70S) SH circulation. Figures 1a and 1b show the climatological zonal-mean zonal wind and its leading EOF, respectively. As discussed by LH01, this mode represents a meridional displacement of the mean jet about its extratropical maximum at 50S. Figures 1c and 1d show a similar analysis for the zonal-mean baroclinicity. We can see that its vertical structure is more complicated than that for zonal wind: while above 800 hPa the maximum baroclinicity is roughly collocated with the wind maximum, the baroclinicity maximum tilts below that level, presumably reflecting the surface forcing. In contrast, the leading mode of variability (23.4% explained variance) has a simple (deep) dipolar structure, suggestive of a meridional shift of baroclinicity about its free troposphere axis. It is noteworthy that the amplitude of the leading mode of baroclinicity variability decays as we go down over the boundary layer and nearly vanishes at the surface, in contrast with the vertical structure of the climatological baroclinicity.

[10] We have also performed an EOF analysis over individual levels. Figure 1e shows the leading baroclinicity EOF at 600 hPa (35.4% variance). This mode again represents a shift of baroclinicity about its maximum, while the second mode (24.8% variance) may be described as a sharpening or broadening of baroclinicity. These are the same two modes that dominate the variability of zonal wind (LH01). Our results are robust for all pressure levels, although the polar lobe of the sine wave becomes distorted and unphysical close to the surface (not shown), where we ignore the seasonality of ice.

[11] Since the dynamics of baroclinic variability might be different at different timescales, we have repeated our analysis at 600 hPa using filtered data. The results are summarized in Table 1. We find that the structure and ranking of the leading two modes is robust when using a low-pass filter, with the separation of the modes increasing (the shift becoming more dominant) as we move to the lower frequencies. In contrast, the two modes explain similar variance (well above the rest of the modes) and are poorly separated when using high-pass filtered data, even when using cutoff periods as long as T = 30 days.

[12] We finally study the relation between barotropic and baroclinic variability. Figure 1f shows the lagged correlation between the principal components (PC) for the leading modes of barotropic (vertically-integrated zonal wind, from the surface to 100 hPa) variability and baroclinic (600 hPa reverse meridional temperature gradient) variability. The correlation is highly significant and reaches its maximum value for small leads of the barotropic PC.

4. Lifecycles of Baroclinic Anomalies

[13] To investigate in more detail the processes driving the variability of baroclinicity we have computed an equation for its leading mode: $B(t) = -\bar{\theta}_y(y,t) \cdot \overrightarrow{EOF}1(y)$, where EOF1 is the first EOF of baroclinicity at 600 hPa (Figure 1e). The equation is obtained differentiating the thermodynamic equation meridionally and projecting the resulting terms onto this EOF. We express it schematically:

$$\frac{\partial B}{\partial t} = F\{\overline{v'\theta'}\} + F\{MMC\} + F\{Heating\} + \{other\,terms\}, \quad (1)$$

where the first three terms on the right hand side reflect the dominant forcings in the thermodynamic equation: the meridional eddy heat flux, the adiabatic heating and cooling in the mean meridional circulation (MMC) and the diabatic heating. This last term was estimated as a residual from the full equation, which also includes additional, much smaller forcings by the eddy vertical heat flux and the MMC meridional advection ('other terms' in equation (1)). For the analysis described below the mean seasonal cycle is subtracted from this equation. (Note that we subtract the mean seasonal cycle of the $\overline{v'\theta'}$ product on the right hand side but use the full, seasonally varying values of v' and θ' to compute this product).

[14] Figure 2a shows the regression of the main forcing terms in equation (1) against the first principal component of baroclinicity, B, as a function of lag. The total tendency (sum of all terms, plotted in black) shows that baroclinic anomalies grow and decay over a characteristic period of 10–15 days. All forcing terms contribute to this tendency though the MMC appears to dominate the eddy heat flux forcing at long lags. The structure of the eddy heat flux forcing is in good agreement with *Stone et al.* [1982], displaying a large, positive peak at negative lags and a smaller, negative peak at positive lags.

[15] A clearer picture emerges when we distinguish between the variability at timescales shorter and longer than 20 days, discriminated by means of a Lanczos filter. In the high frequency (Figure 2b) the eddy heat flux forcing dominates, the MMC forcing is weak and the heating negligible. At these fast timescales, mean baroclinic anomalies essentially respond to variations in the eddy heat flux forcing. The picture is very different in the low frequency range (Figure 2c). For long timescales, baroclinic anomalies are

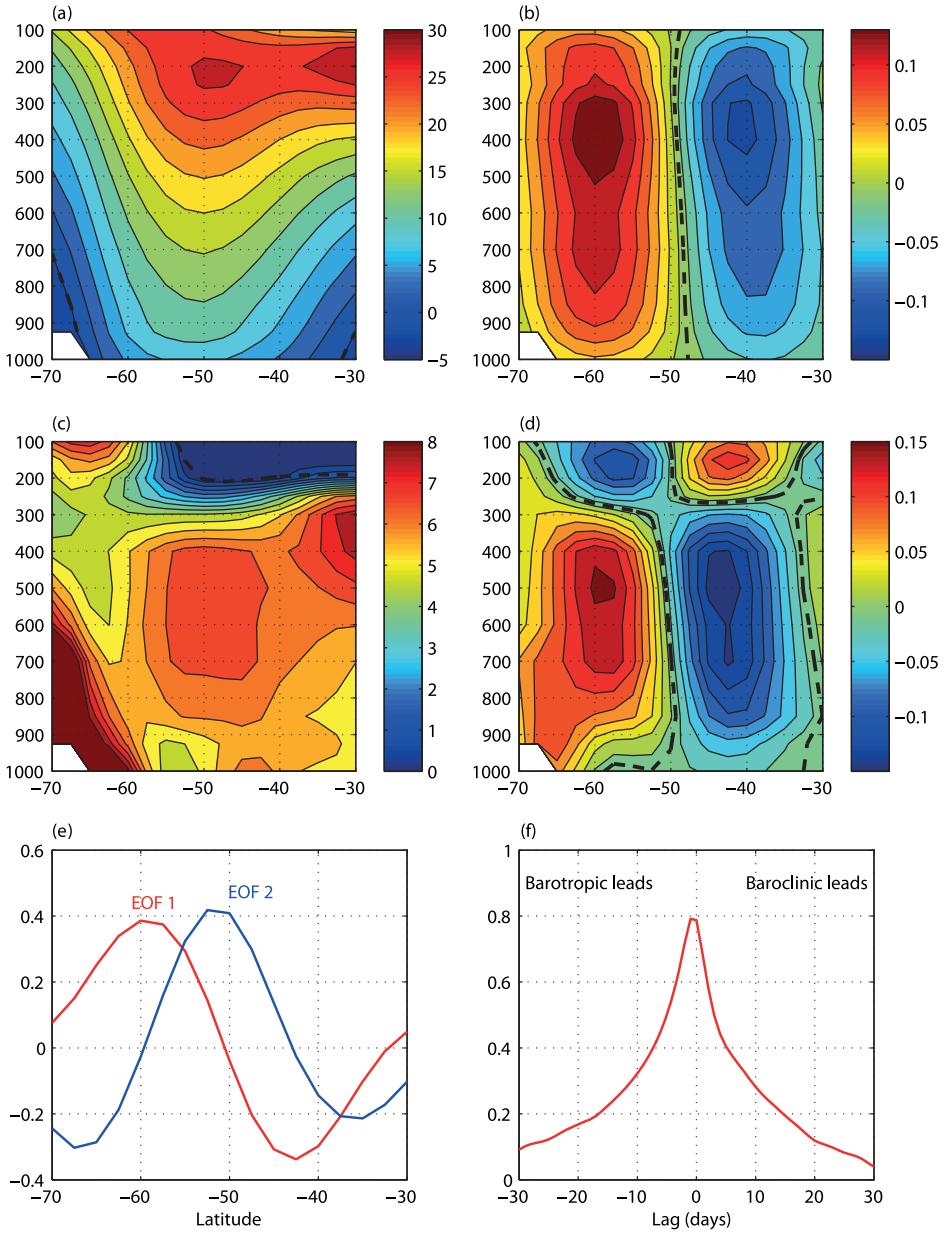

Figure 1. Extratropical SH (30-70S) climatology and variability. (a) Climatological zonal-mean zonal wind in m/s. (b) Its leading EOF. (c) Climatological zonal-mean baroclinicity (reverse meridional potential temperature gradient) in K/1000 km. (d) Its leading EOF. (e) First two EOFs of zonal-mean baroclinicity at 600 hPa. (f) Lagged correlation between the principal components for the leading modes of barotropic and baroclinic variability, with barotropic variability leading at negative lags.

primarily forced by the MMC and damped diabatically. The eddy heat flux is in phase with the total tendency, contributing to the growth of the anomaly and, to a lesser extent, its decay. However, it is clear that this term cannot explain the total tendency. The unfiltered regression (Figure 2a) shows a combination of the high and low frequency results. In particular, the vanishing of the MMC forcing at short lags results from the compensation between low and high frequency forcing, the former driving the baroclinic variability and the latter damping it.

[16] To make sure that the variability described in Figure 2c is not an artifact of the cutoff used in the Lanczos filter, we repeat the analysis using data filtered with a moving average filter. The results are very similar when

Table 1. Percentage Variance Explained by the First and Second Leading EOFs of Zonal-Mean Baroclinicity Variability at 600 hPa, for High- and Low-Pass Filtered Data at Different Frequencies[a]

	Shift	Sharpening
No filter	35.4%	24.9%
10 days 'low'	43.0%	24.9%
30 days 'low'	50.1%	22.0%
90 days 'low'	52.5%	20.2%
10 days 'high'	28.5%	25.4%
30 days 'high'	28.7%	27.2%
90 days 'high'	31.1%	26.6%

[a]The first EOF reflects a shift and the second one a sharpening of baroclinicity except for high-pass filtered, when the modes are poorly separated and may appear merged.

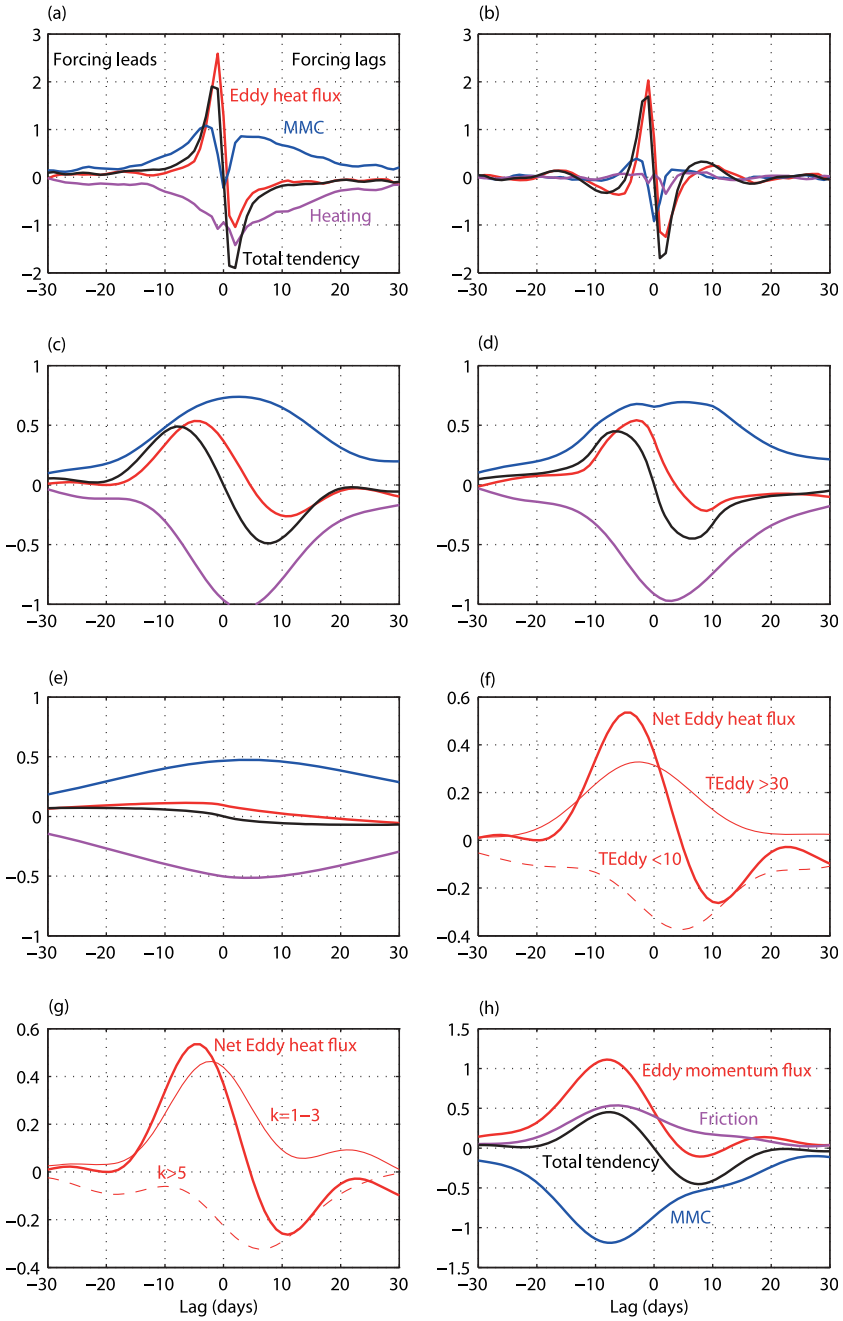

Figure 2. (a) Lagged covariance between zonal-mean baroclinicity and its forcings (eddy heat flux: red, mean meridional circulation: blue, diabatic heating: magenta, total: black), with the forcings leading for negative lags and units expressed in $(K/1000\ km)^2$/day. (b) Same as Figure 2a but for data filtered using a 20-day cutoff high-pass Lanczos filter. (c) Same but for a low-pass 20-day filter. (d) Same but using a 10-day moving average. (e) Same but using a 40-day moving average. (f) Total eddy heat flux forcing (thick, solid) and contributions from high frequency (T_{eddy} <10 days, dashed) and low frequency (T_{eddy} >30 days, solid) eddies. (g) Same but for synoptic ($k \geq 6$, dashed) and planetary scale ($k = 1$-3, solid) eddies. (h) Same as Figure 2a but for vertical shear and the following forcings (eddy momentum flux: red, mean meridional circulation: blue, friction: magenta, total: black).

using a 10-day moving average (Figure 2d). With a 40 day-average (Figure 2e) the variability is smoothed out but qualitatively similar. Our conclusions are not sensitive to the filter used and hold quite generally over a wide range of timescales.

[17] One intriguing aspect in Figure 2c is the sign of the eddy heat flux forcing, as one might expect baroclinic instability to damp the zonal-mean baroclinic anomalies on timescales longer than the characteristic temporal scale of the eddies. However, it should be borne in mind that the eddy heat flux forcing in equation (1) includes contributions from eddies of all temporal and spatial scales. Figure 2f separates the contributions to this term from eddies with periods shorter than 10 days and longer than 30 days (now also filtering the v' and θ' time series prior to computing the eddy covariances) and Figure 2g separates the contributions

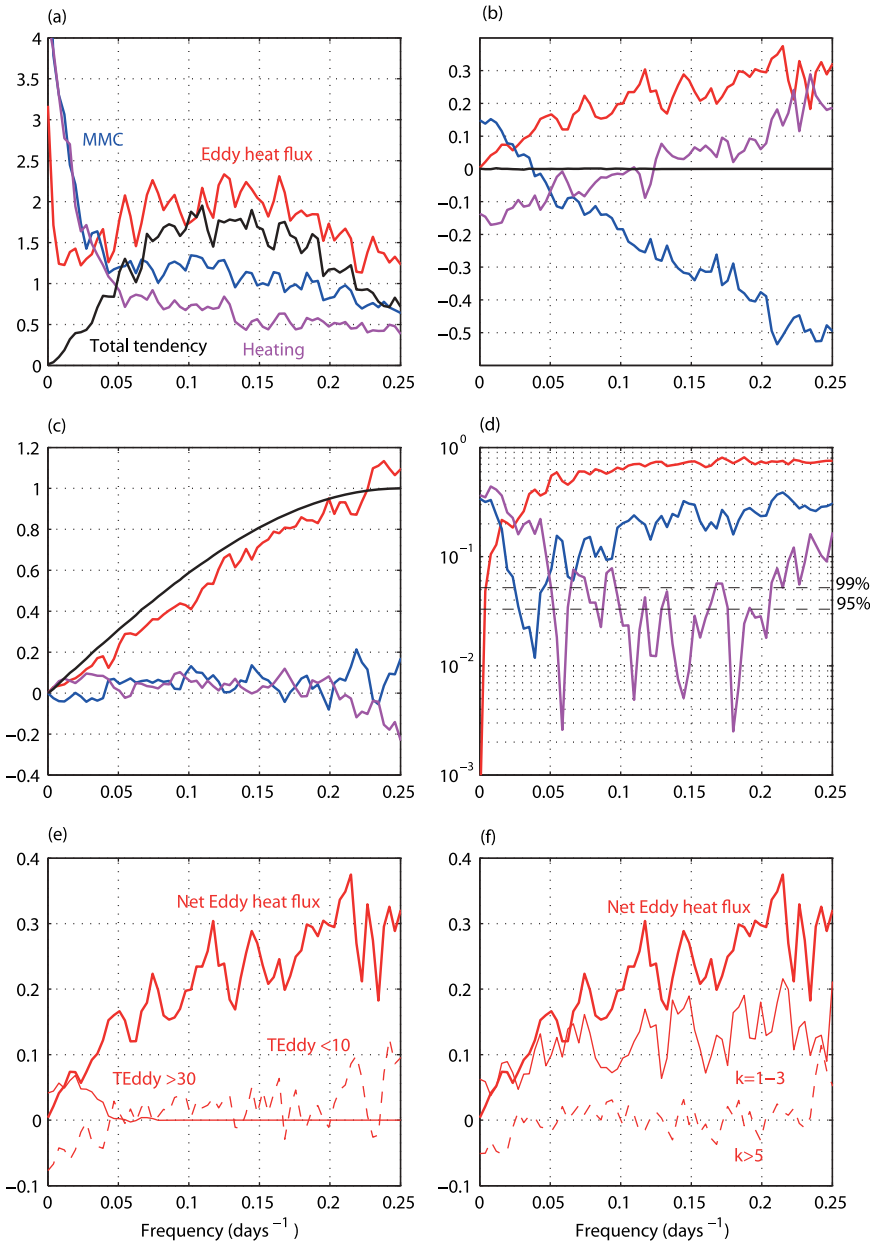

Figure 3. (a) Power spectra of all forcing terms in the baroclinicity equation (eddy heat flux: red, mean meridional circulation: blue, diabatic heating: magenta, total tendency: black), expressed in $(K/1000\ km)^2$. (b) Normalized real cospectrum $\mathrm{Re}\left[\widetilde{F}\widetilde{B}^*\right]/\widetilde{B}^*\widetilde{B}$ in $days^{-1}$. (c) Imaginary cospectrum $\mathrm{Im}\left[\widetilde{F}\widetilde{B}^*\right]/\widetilde{B}^*\widetilde{B}$ in $days^{-1}$. (d) Squared spectral coherence. (e) As Figure 3b but for the total eddy heat flux forcing (thick, solid) and the contributions from high frequency (T_{eddy} <10 days, dashed) and low frequency (T_{eddy} >30 days, solid) eddies. (f) Same but for synoptic (k ≥ 6, dashed) and planetary scale (k = 1-3, solid) eddies.

from planetary (k = 1-3) and synoptic (k ≥ 6) eddies. It is apparent that the positive forcing in Figure 2c is due to the low-frequency planetary eddies, while synoptic scale eddies tend on average to damp the baroclinicity anomalies. The planetary eddy heat transport presumably reflects the slow, seasonal evolution of the quasi-stationary circulation over Antarctica.

[18] Finally, we can get a better grasp on the origin of the MMC forcing by performing a similar analysis for the leading mode of vertical shear variability: $S = (\Theta_0/g)f\bar{U}_z \cdot \overrightarrow{EOF}_1$, where f is the latitude-dependent Coriolis parameter, $\bar{U}_z$ is the vertical wind shear and the remaining parameters are constants. Note that B and S would be exactly equal if the thermal wind relation were precisely satisfied. We can obtain an equation for S differentiating the zonal momentum equation at 600 hPa vertically and projecting its terms onto the leading vertical shear EOF. This is identical to the first baroclinicity EOF, and the corresponding PCs are also very highly correlated (97.1%). The equation for S may be expressed:

$$\frac{\partial S}{\partial t} = F\{\overline{u'v'}\} + F\{MMC\} + F\{Friction\} \qquad (2)$$

The MMC term now reflects the creation of vertical shear by the Coriolis force acting on the mean meridional circulation and the frictional term is evaluated as a residual. As before, the seasonal cycle is subtracted from all terms in this balance.

[19] Figure 2h shows the lagged correlation between S and its different forcing terms for data low-pass filtered using a 20-day cutoff Lanczos filter. Because the thermal wind relation is well satisfied, the total tendencies (black lines) in Figures 2c and 2h are quite similar. Figure 2h shows that vertical wind shear anomalies are initially created by the eddy momentum flux forcing, which is top-trapped, and enhanced and extended by the frictional forcing. The vertical shear anomaly is ultimately damped by the MMC forcing. It is noteworthy that the peak in the momentum flux forcing precedes all other peaks in the B lifecycle (Figure 2c).

[20] Putting the results of Figures 2c and 2h together, the low-frequency lifecycles may be described as follows: (i) Vertical shear anomalies are created by the upper troposphere eddy momentum flux and strengthened by surface friction. (ii) An indirect MMC is driven, which weakens the shear anomaly and forces a baroclinicity anomaly to maintain thermal wind balance in the presence of the momentum forcing. iii) The baroclinicity anomaly is damped diabatically. There is also a net, positive eddy heat flux forcing of baroclinicity due to the planetary eddies, which exceeds the negative heat flux forcing by the synoptic eddies.

5. Spectral Analysis

[21] An alternative approach for investigating the sensitivity to frequency is by means of a spectral analysis. Figure 3a shows the power spectra of the forcing terms in equation (1). The eddy heat flux forcing has a fairly flat spectrum and is the dominant term for most frequencies but the MMC and diabatic forcing have redder spectra and dominate at low frequency.

[22] We can also take the Fourier transform of equation (1) to obtain:

$$i\omega = \sum_k \frac{\widetilde{F}_k \widetilde{B}^*}{\widetilde{B}\widetilde{B}^*}, \tag{3}$$

where the tilde denotes a Fourier transform and the asterisk a complex conjugate. The $\widetilde{F}_k$ terms represent the Fourier transform of the forcing terms on the right hand side of equation (1) and ω denotes frequency. This equation shows that the imaginary part of the complex cospectrum between $\widetilde{F}_k$ and $\widetilde{B}$ contributes to the oscillation of the anomaly, whereas the real part makes its amplitude grow (for positive $\mathrm{Re}\left[\widetilde{F}_k \widetilde{B}^*\right]$) or decay (when it is negative).

[23] Figures 3b and 3c show the real and imaginary part of the $\widetilde{F}_k \widetilde{B}^* / \widetilde{B}\widetilde{B}^*$ terms as a function of frequency and Figure 3d the associated squared spectral coherence, which exceeds 95% and 99% significance levels for most frequencies. It is noteworthy that $\mathrm{Re}\left[\widetilde{F}\{\overline{v'\theta'}\}\widetilde{B}^*\right]$ remains positive at all frequencies, which implies that the total eddy heat flux forcing varies in phase with the baroclinicity and always makes it grow, consistent with Figure 2. However, this again reflects compensating effects by planetary and synoptic eddies, the former being dominant at low frequency (Figures 3e and 3f). While the real cospectrum of the low-frequency, planetary eddy heat flux forcing is positive definite, the real cospectrum of the synoptic eddy forcing changes sign and becomes negative at low frequency, implying a damping behavior for the eddy heat flux.

6. Discussion

[24] While the maintenance of extratropical baroclinicity has been traditionally understood as a competition between diabatic heating and transient eddy heat flux forcing, some more recent theoretical work has suggested that the eddy momentum fluxes may also be important in the time dependent problem [*Robinson*, 2000]. Motivated by these ideas, our study has aimed to describe the internal variability of baroclinicity and dissect its driving forces using Southern Hemisphere data. We found that the leading mode of variability for baroclinicity consists of a meridional shift at all timescales, but the dynamics of this shift is very different depending on frequency. While at high frequency the growth and decay of the baroclinicity anomalies essentially respond to variations in the eddy heat flux forcing, at low frequency baroclinic anomalies are forced by the eddy momentum flux and surface friction through an eddy-driven mean meridional circulation, and damped diabatically.

[25] The important role of diabatic heating for damping the low frequency baroclinic anomalies may be surprising. We suspect that this term may reflect the strong thermal damping near the ocean surface, which relaxes the surface air temperature in timescales as short as a day [*Swanson and Pierrehumbert*, 1997]. *Nakamura et al.* [2004] have emphasized the role of air-sea heat exchange in anchoring the surface baroclinicity to the underlying SST front over the oceanic stormtracks and several modeling studies have shown that the midlatitude SST gradients exert a strong influence on the climatological baroclinicity and stormtrack activity [*Nakamura et al.*, 2008; *Brayshaw et al.*, 2008]. By strongly restoring the mean baroclinicity, air-sea heat exchange should also damp its variability. It is telling in this regard that the amplitude of the leading baroclinicity EOF decays over the boundary layer, in contrast with the mean baroclinicity (Figure 1). Latent heating has been found to affect zonal-index persistence in idealized studies [*Xia et al.*, 2011] and may also be important.

[26] Our results support the hypothesis of *Robinson* [2000] that the eddy momentum flux and friction play an important role for the variability of baroclinicity during the zonal index cycle, consistent with some recent observational and modeling evidence [*Kidston et al.*, 2010; *Chen and Plumb*, 2009]. *Robinson* [2000] also argues that this baroclinicity forcing contributes to enhancing the zonal index persistence due to the anomalous eddy generation and eddy-induced acceleration over the region of anomalous baroclinicity. However, some recent modeling studies have suggested that barotropic dynamics alone can produce realistic zonal index variability [*Barnes et al.*, 2010]. More research is needed to elucidate whether the baroclinic feedback proposed by *Robinson* [2000] plays any role in enhancing the persistence of the zonal index.

[27] **Acknowledgments.** This work was supported by the MOVAC project (grant 200800050084028 of the Ministerio de Medio Ambiente, y Medio Rural y Marino of Spain) and by grant CGL2009-06944 from the Ministerio de Ciencia e Innovación of Spain.

[28] The Editor thanks the two anonymous reviewers for their assistance in evaluating this paper.

References

Barnes, E. A., D. L. Hartmann, D. M. W. Frierson, and J. Kidston (2010), The effect of latitude on the persistence of eddy-driven Jets, *Geophys. Res. Lett.*, *37*, L11804, doi:10.1029/2010GL043199.

Brayshaw, D. J., B. Hoskins, and M. Blackburn (2008), The storm-track response to idealized SST perturbations in an aquaplanet GCM, *J. Atmos. Sci.*, *65*, 2842–2860, doi:10.1175/2008JAS2657.1.

Chen, G., and R. A. Plumb (2009), Quantifying the eddy feedback and the persistence of the zonal index in an idealized atmospheric model, *J. Atmos. Sci.*, *66*, 3707–3720, doi:10.1175/2009JAS3165.1.

Hamming, R. W. (1989), *Digital Filters*, Prentice Hall, Englewood Cliffs, N. J.

Hartmann, D. L. (1994), *Global Physical Climatology*, Academic, San Diego, Calif.

Held, I. M., and V. D. Larichev (1996), A scaling theory for horizontally homogeneous, baroclinically unstable flow on a beta plane, *J. Atmos. Sci.*, *53*, 946–952, doi:10.1175/1520-0469(1996)053<0946:ASTFHH>2.0.CO;2.

Hoskins, B. J., and P. J. Valdes (1990), On the existence of storm-tracks, *J. Atmos. Sci.*, *47*, 1854–1864, doi:10.1175/1520-0469(1990)047<1854:OTEOST>2.0.CO;2.

Kalnay, E., et al. (1996), The NCEP/NCAR 50-year reanalysis project, *Bull. Am. Meteorol. Soc.*, *77*, 437–471, doi:10.1175/1520-0477(1996)077<0437:TNYRP>2.0.CO;2.

Kanamitsu, M., W. Ebisuzaki, J. Woollen, S.-K. Yang, J. J. Hnilo, M. Fiorino, and G. L. Potter (2002), NCEP-DOE AMIP-II Reanalysis (R-2), *Bull. Am. Meteorol. Soc.*, *83*, 1631–1643, doi:10.1175/BAMS-83-11-1631.

Kidston, J., D. M. W. Frierson, J. A. Renwick, and G. K. Vallis (2010), Observations, simulations, and dynamics of jet stream variability and annular modes, *J. Clim.*, *23*, 6186–6199, doi:10.1175/2010JCLI3235.1.

Lindzen, R. S., and B. Farrell (1980), A simple approximate result for the maximum growth rate of baroclinic instabilities, *J. Atmos. Sci.*, *37*, 1648–1654, doi:10.1175/1520-0469(1980)037<1648:ASARFT>2.0.CO;2.

Lorenz, E. N. (1955), Available potential energy and the maintenance of the general circulation, *Tellus*, *7*, 157–167, doi:10.1111/j.2153-3490.1955.tb01148.x.

Lorenz, E. N. (1979), Forced and free variations of weather and climate, *J. Atmos. Sci.*, *36*, 1367–1376, doi:10.1175/1520-0469(1979)036<1367:FAFVOW>2.0.CO;2.

Lorenz, D. J., and D. L. Hartmann (2001), Eddy–zonal flow feedback in the Southern Hemisphere, *J. Atmos. Sci.*, *58*, 3312–3327, doi:10.1175/1520-0469(2001)058<3312:EZFFIT>2.0.CO;2.

Nakamura, H., T. Sampe, Y. Tanimoto, and A. Shimpo (2004), Observed associations among storm tracks, jet streams and midlatitude oceanic fronts, in *Earth's Climate: The Ocean-Atmosphere Interaction*, *Geophys. Monogr. Ser.*, vol. 147, edited by C. Wang, S.-P. Xie, and J. A. Carton, pp. 329–345, AGU, Washington, D. C., doi:10.1029/147GM18.

Nakamura, H., T. Sampe, A. Goto, W. Ohfuchi, and S.-P. Xie (2008), On the importance of midlatitude oceanic frontal zones for the mean state and dominant variability in the tropospheric circulation, *Geophys. Res. Lett.*, *35*, L15709, doi:10.1029/2008GL034010.

Robinson, W. A. (2000), A baroclinic mechanism for the eddy feedback on the zonal index, *J. Atmos. Sci.*, *57*, 415–422, doi:10.1175/1520-0469(2000)057<0415:ABMFTE>2.0.CO;2.

Robinson, W. A. (2006), On the self-maintenance of midlatitude jets, *J. Atmos. Sci.*, *63*, 2109–2122, doi:10.1175/JAS3732.1.

Simmons, A. J., and B. J. Hoskins (1978), The life cycles of some nonlinear baroclinic waves, *J. Atmos. Sci.*, *35*, 414–432, doi:10.1175/1520-0469(1978)035<0414:TLCOSN>2.0.CO;2.

Stone, P. H., and D. A. Miller (1980), Empirical relations between seasonal changes in meridional temperature gradients and meridional fluxes of heat, *J. Atmos. Sci.*, *37*, 1708–1721, doi:10.1175/1520-0469(1980)037<1708:ERBSCI>2.0.CO;2.

Stone, P. H., S. J. Ghan, D. Spiegel, and S. Rambaldi (1982), Short-term fluctuations in the eddy heat flux and baroclinic stability of the atmosphere, *J. Atmos. Sci.*, *39*, 1734–1746, doi:10.1175/1520-0469(1982)039<1734:STFITE>2.0.CO;2.

Swanson, K. L., and R. T. Pierrehumbert (1997), Lower-tropospheric heat transport in the Pacific storm track, *J. Atmos. Sci.*, *54*, 1533–1543, doi:10.1175/1520-0469(1997)054<1533:LTHTIT>2.0.CO;2.

Thompson, D. W. J., and J. M. Wallace (2000), Annular modes in the extratropical circulation. Part I: Month-to-month variability, *J. Clim.*, *13*, 1000–1016, doi:10.1175/1520-0442(2000)013<1000:AMITEC>2.0.CO;2.

Xia, X., Y. Guo, and E. K. M. Chang (2011), Diabatic damping of zonal index variations, paper presented at 18th Conference on Atmospheric and Oceanic Fluid Dynamics, Am. Meteorol. Soc., Spokane, Wash.

J. Blanco-Fuentes and P. Zurita-Gotor, Departamento de Geofísica y Meteorología, Facultad de Ciencias Físicas, Universidad Complutense de Madrid, Ciudad Universitaria s/n, E-28040 Madrid, Spain. (pzurita@alum.mit.edu)